

# Dynamic Access and Power Control Scheme for Interference Mitigation in Femtocell Networks

**Mujeeb Ahmed<sup>1</sup> and Sung-Guk Yoon<sup>2</sup>**

<sup>1</sup>Information Systems Technology and Design,  
Singapore University of Technology and Design, Singapore  
[e-mail:chuadhry@mymail.sutd.edu.sg]

<sup>2</sup>School of Electrical Engineering,  
Soongsil University, Seoul, Korea  
[e-mail: sgyoon@ssu.ac.kr]

\*Corresponding author: Sung-Guk Yoon

*Received May 11, 2015; revised August 11, 2015; accepted September 13, 2015;  
published November 30, 2015*

---

## Abstract

The femtocell network, which is designed for low power transmission and consists of consumer installed small base stations, coexists with macrocells to exploit spatial reuse gain. For its realization, cross-tier interference mitigation is an important issue. To solve this problem, we propose a joint access and power control scheme that requires limited information exchange between the femto and macro networks. Our objective is to maximize the network throughput while satisfying each user's quality of service (QoS) requirement. To accomplish this, we first introduce two distributed interference detection schemes, i.e., the femto base station and macro user equipment based schemes. Then, the proposed scheme dynamically adjusts the transmission power and makes a decision on the access mode of each femto base station. Through extensive simulations, we show that the proposed scheme outperforms earlier works in terms of the throughput and outage probability.

---

**Keywords:** Access control, femtocell, interference mitigation, power control

## 1. Introduction

**R**ecent survey from Cisco [1], shows that in 2019 mobile data traffic will attain 24.3 exabytes per month. By anticipating the challenge posed by this data traffic explosion and the fact that 90% of data services originate from indoors, femtocell networks have been proposed to cover small indoor areas. Femtocells are a prominent and efficient solution to increase throughput and to extend cell coverage especially for cell edge and indoor areas in which the signal strength of macro base station is normally weak. In the future, femtocells will be deployed in large numbers by end users. These femtocells will be deployed without any cell planning; therefore, integrating femtocell networks with existing networks is a major technical challenge [2].

For the deployment of femto networks, cross-tier interference is an important problem to solve. For instance, when a macro user equipment (MUE) is close to a femto base station (FBS), the MUE could experience outage due to the interfering signal from the FBS. Similarly, during uplink transmission, the MUE imparts strong interference to the femtocell. This is known as the “loud neighbor problem,” which becomes more critical when the MUE is at the cell edge or far from the macro base stations (MBSs) [3].

To solve the cross-tier interference problem, extensive research has been done. Among these schemes which have been proposed, some apply the concept of fractional frequency reuse to avoid cross-tier interference for both macrocells and femtocells [4], [5]. Others have proposed using downlink power control to manage the interference level [6]-[8]. In [6], [7], FBSs reduce their transmission powers according to the received MBS power. These schemes, however, rely on an approximated interference measure to adjust the transmission power of the FBS. The authors in [8] have proposed a downlink power control scheme using Stackelberg game, which assumed that the MBS and FBSs are leader and followers, respectively.

A distributed downlink power control scheme has been proposed in [9], where femtocells generating strong interference are discouraged from using a high power level. In [10], a cognitive radio based interference coordination framework has been proposed to estimate and to mitigate the cross-tier interference. The authors in [11], described three access control schemes that can be used in femtocell networks; the closed access (where access is granted to subscribed users only), open access (where access is granted to any user within the coverage area) and hybrid access (which is a combination of closed and open access) schemes. In [12], the performances of the open and closed access schemes have been compared. Ping et al. [13] carried out a study on open versus closed access schemes for various medium access technologies. Another work has compared the tradeoff between spectrum and energy efficiency in two-tier femtocell networks using partially open channels [14].

Our objective in this paper is to maximize the network-wide user throughput while satisfying the signal to interference plus noise ratio (SINR) constraints of neighboring MUEs, FBSs and FUEs by controlling the FBS's access mode and transmission power. To this end, we first formulate this as a problem of maximizing the network-wide user throughput. Then, we divide the problem into two subproblems: the access mode and transmission power subproblems. Since the algorithm which we propose to solve the optimization algorithm runs at the MBS in a centralized manner and requires a lot of information, we also propose a simple local search algorithm that runs at each FBS in a distributed manner. The local search algorithm detects interference first and applies a rule based algorithm for simple operation.

Through extensive simulations, we show that the proposed scheme outperforms earlier works in terms of the throughput since the proposed interference detection scheme is more accurate and adjusts both the access mode and transmission power.

The remainder of the paper is organized as follows. In Section 2, we present a system model for the cross-tier interference problem. The network-wide user throughput maximization problem and its suboptimal solution are described in Section 3. Then, we propose two distributed interference detection methods and a heuristic local search algorithm for the optimization problem in Section 4. In Section 5, we evaluate the system performance through simulations and numerical method. Finally, we conclude our work in Section 6.

## 2. System Model

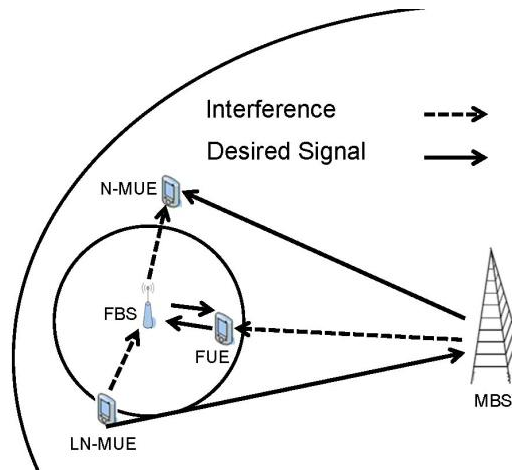


Fig. 1. System model

We consider an orthogonal frequency-division multiple access (OFDMA) based system with  $BW$  MHz bandwidth. There is one MBS and many FBSs in the network. We assume that the MBS and FBSs both use the  $BW$  MHz bandwidth, i.e., co-channel deployment<sup>1</sup>. User equipments (UEs) subscribed to the MBS and FBSs are referred to as MUEs and FUEs, respectively. MUEs that interfere with an FBS for downlink and uplink are called neighboring MUEs (N-MUEs) and loud neighbor MUEs (LN-MUEs), respectively. We assume that the coverage area of each FBS and MBS is circular for the sake of simplicity. The coverage of an FBS could vary according to the transmission power. It is assumed that all UEs and BSs are equipped with omnidirectional transmit and receive antennas. Femtocells are sparsely distributed across the macro area, so inter-femto interference is ignored. We assume that FUEs and MUEs are static or moving at pedestrian walking speed, i.e., 1.3 m/s [15], in the network. Fig. 1 shows an example of the networks considered herein. There are one MBS and one FBS serving two MUEs and one FUE, respectively. One MUE is interfered with by the FBS, and the other MUE interferes with the FBS, which are referred to as the N-MUE and LN-MUE, respectively.

We define  $U_F$  and  $U_M$  as the sets of FUEs and MUEs, respectively.  $B_F$  is the set of FBSs in the considered system. A UE is only associated with a single BS at a time. The

<sup>1</sup> The proposed scheme is not limited to a single channel system. In the multichannel system, the proposed scheme can be applied to each subchannel independently.

channel gains from FUE  $f$  to FBS  $F$  and MBS  $M$  are expressed as  $h_f^F$  and  $h_f^M$ , respectively. Similarly, the channel gains from MUE  $m$  to MBS  $M$  and FBS  $F$  are  $h_m^M$  and  $h_m^F$ , respectively<sup>2</sup>. We assume a reciprocal channel for the uplink and downlink between a UE and its serving BS.

It is assumed that an FUE does not cause interference with the MBS for uplink when it transmits at low power, while the MUEs interfere with the FBSs. The SINR at FBS  $F$  associated with FUE  $f$ , i.e., on the uplink, can be expressed as

$$\gamma_F^f = \frac{p_f |h_f^F|^2}{\sum_{m \in U_M} p_m |h_m^F|^2 + N_o}, \quad (1)$$

where  $p_f$  and  $p_m$ , are the transmission powers of the FUE and MUE, respectively, and  $N_o$  is the noise spectral density. The SINR at FBS  $F$  is defined by  $\gamma_F = \min \gamma_F^f$  for all FUEs associated with  $F$ . Conversely, the SINR at FUE  $f$  associated with FBS  $F$ , i.e., on the downlink, can be expressed as

$$\gamma_f^F = \frac{p_f |h_f^F|^2}{p_M |h_f^M|^2 + N_o}, \quad (2)$$

where  $p_M$  is the transmission power of the MBS. Since we ignore inter femto interference, only that of the MBS is considered at the FUE. Similarly, the SINR at MUE  $m$  associated with MBS  $M$  can be expressed as

$$\gamma_m^M = \frac{p_M |h_m^M|^2}{\sum_{F \in B_f} p_F |h_m^F|^2 + N_o}, \quad (3)$$

where  $p_F$  is the transmit power of FBS  $F$ . Although our system model considers environments with a single channel and single MBS, it can be easily extended to the multichannel multicell case.

While the channel gains  $h_f^F$  and  $h_f^M$  can be directly obtained from the FUE's feedback to its associated FBS,  $h_m^M$  and  $h_m^F$  cannot because there is no direct feedback channel for cross-tier information exchange. To allow this to happen, cross-tier feedback between MBS and FBS is needed through the backhaul network. We assumed that each FBS is connected with the core network through the Internet. Then, MBS and FBS can communicate each other by using the Internet, that is, backhaul link for FBS.

### 3. Problem Formulation and Suboptimal Solution

In this section, we numerically formulate a network-wide user throughput maximization problem and derive a suboptimal solution.

<sup>2</sup> The channel gains are mainly affected by the path-loss in this paper. We assume that there is no fast fading. However, when the channel gain is changed due to the location changes of the users or shadowing, the proposed algorithm (Section 4.2) is initiated by the interference detection method (Section 4.1).

### 3.1 Problem Formulation

The objective of our joint access and power control scheme is to maximize the network-wide user throughput while satisfying the quality of service (QoS) requirements in terms of the SINR. That is,

$$\max_{p_F; A_m} \left[ \sum_{f \in U_F} C_f^F + \sum_{m \in U_M} ((1 - A_m)C_m^M + A_m C_m^F) \right], \quad (4)$$

subject to

$$\gamma_m > \gamma_{th,m}, \quad \forall m \in U_M, \quad (5a)$$

$$\gamma_f > \gamma_{th,f}, \quad \forall f \in U_F, \quad (5b)$$

$$\gamma_F > \gamma_{th,F}, \quad \forall F \in B_F, \quad (5c)$$

$$p_{min,F} \leq p_F \leq p_{max,F}, \quad \forall F \in B_F \quad (5d)$$

where  $A_m$  denotes an FBS association indicator of MUE  $m$ . If  $A_m = 1$ ,  $m$  is associated with FBS. If  $A_m = 0$ ,  $m$  is associated with MBS. The throughput of UE  $u$  associated with BS  $B$  (either FBS or MBS) can be given as  $C_u^B = BW \log_2(1 + \gamma_u^B) \frac{G(N)}{N}$ , where  $BW$  is the total bandwidth,  $N$  is the number of UEs associated with BS  $B$ , and  $G(N)$  indicates the scheduling factor. Since  $A_m$  is an integer and  $p_F$  is real, this optimization problem is a mixed-integer programming problem that is generally known to be NP-hard.

### 3.2 Suboptimal Solution

To solve this problem, we divide it into two subproblems and solve them one after the other. The first subproblem is an access control one (selecting  $A_m$  with constant  $p_F$ ) and the second involves optimizing the FBS transmission power (selecting  $p_F$  with fixed  $A_m$ ).

The first subproblem is a kind of Knapsack problem. A Knapsack problem is an assignment problem of combinatorial optimization. We have a set of macro users  $U_M$ , where each user  $m$  has a throughput function  $C_m$  and a weight  $w_m$ , i.e., the amount of bandwidth assigned to user  $m$ . The whole required bandwidth should be less than the available resource  $W_{a,F}$  [16]. We can formulate a bounded 0-1 Knapsack problem as a linear integer program [17]. That is,

$$\max_{A_m} \left[ \sum_{m \in U_M} ((1 - A_m)C_m^M + A_m C_m^F) \right], \quad (6)$$

subject to

$$\sum_{m \in U_M} w_m A_m \leq W_a, \quad (7a)$$

$$\gamma_F > \gamma_{th,F}, \quad \forall F \in B_F, \quad (7b)$$

$$A_m \in \{0, 1\}, \quad \forall m \in U_M, \quad (7c)$$

where  $W_a = (BW_F - BW_{req})$  represents the available bandwidth obtained by subtracting the FUE's bandwidth requirement ( $BW_{req}$ ) from the achievable bandwidth ( $BW_F$ ) for each FBS. When an FBS opens the access, it should have some available bandwidth, i.e.,

$BW_F - BW_{req} \geq 0, \forall F \in B_F$ . Some N-MUEs are accepted by the FBS, whereas the others are still associated with the MBS. The accepted N-MUEs become FUEs. To solve this Knapsack problem, we use a binary integer program employing branch and bound algorithm [18]. Branch and bound algorithm is a method of solving combinatorial problems. It maintains provable lower and upper bounds on a global objective value and which can be found using convex relaxation and a local optimization method, respectively.

Now, we formulate the transmission power optimization problem with fixed  $A_m$ . We have

$$\max_{p_F} \left[ \sum_{f \in U_F} C_f^F + \sum_{m \in U_M} C_m^M \right], \quad \forall F \in B_F, \quad (8)$$

subject to

$$\gamma_m > \gamma_{th,m}, \quad \forall m \in U_M, \quad (9a)$$

$$\gamma_f > \gamma_{th,f}, \quad \forall f \in U_F, \quad (9b)$$

$$p_{min,F} \leq p_F \leq p_{max,F}, \quad \forall F \in B_F. \quad (9c)$$

This objective function is still non convex with respect to  $p_F$ , so it is hard to find a global optimum [6], [17], [19]. To obtain a suboptimal solution for this problem, an interior point method [20] is used. The overall problem structure is presented in Fig. 2.

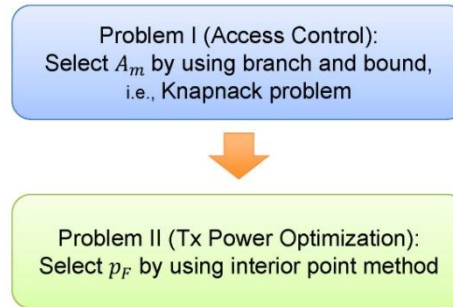


**Fig. 2.** To get a suboptimal solution, the original problem is divided into two subproblems and we solve them one by one.

We refer to this suboptimal solution as KP-IP, which stands for Knapsack problem and interior point method. Although we can obtain a suboptimal solution for the original problem by solving the two subproblems, this algorithm runs in a centralized manner and requires all of the channel gains of the UEs in the network to be known. This is not a practical assumption.

Note that the suboptimal solution is always a feasible solution to the original optimization problem since it satisfies all the constraints of the original problem.

### 3.3 Computational Complexity

We analyze the computational complexity of the KP-IP algorithm. A binary integer program used to solve the Knapsack problem has computational complexity of order  $O(2^{m+1})$ , where  $m$  is the number of neighboring FBSs close to the MUE and 1 is added to count for the single MBS in the network [17]. For the interior point method we used the LDL-factorization<sup>3</sup>

<sup>3</sup> LDL is a variant of classical Cholesky decomposition. It consists of three matrix that are Lower triangular matrix, Diagonal matrix, and Hermitian of the Lower triangular matrix.

algorithm, which takes  $O(n^3)$  computations, where  $n$  is the number of FBSs in the whole network [21]. Combining these two, the complexity of the KP-IP algorithm is  $O(2^{m+1}) + O(n^3)$ .

### 4. Proposed Joint Access and Power Control Scheme

We propose a heuristic algorithm that runs at each FBS in a distributed manner. The proposed algorithm consists of two parts: interference detection and rule based decision.

#### 4.1 Interference Detection Methods

To improve the network wide throughput and minimize the cross-tier interference, we need information about the interferers, namely their channel gains, their interference levels and so on. We propose two indirect feedback mechanisms to obtain information about the N-MUEs (downlink) and LN-MUEs (uplink) which may be triggered either simultaneously or separately.

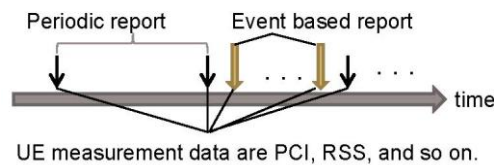


Fig. 3. UE measurement report. “Periodic report” and “Event based report” stand for LTE standard report and the proposed report method, respectively [22].

In an LTE cellular network, a UE sends measurement reports periodically to the MBS which include the physical cell ID (PCI) of each neighbor cell and its received signal strength (RSS) [23], while the MBS maintains a measurement table for each user. Fig. 3 shows these report procedures in time where the event based reports represent the reports activated by the proposed method.

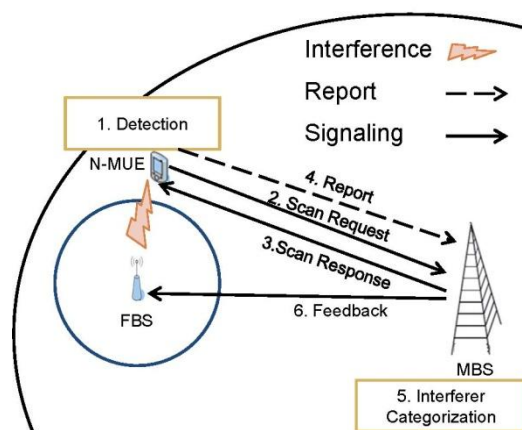


Fig. 4. N-MUE feedback based detection method

i) **N-MUE Feedback based Detection Method (NDM)**: The event based reports can be activated by the following N-MUE based detection method (NDM). Fig. 4 shows an example

of an NDM. In this example, the suffering N-MUE initiates the NDM. The steps of this algorithm are as follows.

- 1) Detection: An N-MUE detects an interferer when its SINR falls below a certain threshold level.
- 2) Scan Request: The N-MUE sends the scan request to the MBS to get permission to scan the air.
- 3) Scan Response: The MBS replies to the N-MUE with the permission to scan (scan response message).
- 4) Report: The N-MUE sends its channel scanning report to the MBS, which contains all the neighbor's PCIs and their respective RSSs.
- 5) Interferer Categorization: The MBS categorizes the MUEs according to their interference levels obtained from the N-MUE's report.
- 6) Feedback: The MBS gives a feedback message to the respective FBS for coordination through the backhaul, which contains the MUE's ID and RSSs ( $h_m^M$  and  $h_m^F$ ).

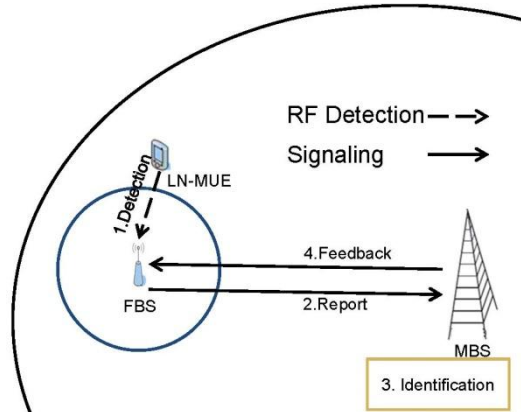


Fig. 5. FBS feedback based detection method

**ii) FBS Feedback based Detection Method (FDM):** Although the channel is assumed to be reciprocal, the interference levels of the uplink and downlink are different due to the various positions of the MUEs. Therefore, the FBS also has its own interference detection method. The detailed procedures based on the feedback from the FBS are shown in Fig. 5. The steps are as follows.

- 1) Detection: The FBS detects the existence of an MUE when its SINR falls below a certain threshold level.
- 2) Report: Through the backhaul, the FBS reports this information to the MBS that contains its physical cell ID (PCI) information.
- 3) Identification: The MBS checks the FBS report from all of the MUEs. When a PCI match occurs, the MBS can track the LN-MUE of interest.
- 4) Feedback: The feedback message from the MBS to FBS is sent through the backhaul. It contains the information about the LN-MUE's ID and RSSs ( $h_m^M$  and  $h_m^F$ ).

#### 4.2 Adaptive Rule based Local Search Algorithm (ARLSA)

Through the above detection methods, an FBS obtains the channel gain of the MUE, i.e.,  $h_m^M$  and  $h_m^F$ , and the FBS already knows the channel gains of the FUE, i.e.,  $h_f^F$  and  $h_f^M$ . With



this channel information, the FBS controls the access and power for the purpose of improving the network-wide user throughput. We propose a heuristic algorithm called adaptive rule based local search algorithm (ARLSA). Since the FBSs only know their local information, we refer to our algorithm as a local search. It is an iterative search technique to find a local solution. To lower the complexity, we use a rule set [24]. According to the constraints in (5), we build an action space as shown in **Table 1**. Here, ‘O’ means that the respective constraint is satisfied, while ‘X’ means it is not. PC and OA in the table mean power control and open access, respectively.

**Table 1.** Ruleset for local search algorithm

State	$\gamma_m > \gamma_{th,m}$	$\gamma_f > \gamma_{th,f}$	$\gamma_F > \gamma_{th,F}$	Action Space
$\beta$	O	O	O	None
A	O	O	X	OA
B	O	X	O	PC
C	O	X	X	OA and PC
D	X	O	O	PC
E	X	O	X	OA and PC
F	X	X	O	OA and PC
G	X	X	X	OA and PC

**Algorithm 1.** ARLSA

```

1:  $A_m \leftarrow 0, \forall m \in U_M$ ; // initialization
2: while infinite loop do
3:   if  $\gamma_m < \gamma_{th,m}$  or  $\gamma_F < \gamma_{th,F}$  then
4:     if  $\gamma_m < \gamma_{th,m}$  then
5:       Get  $h_m^M, h_m^F$  through NDM;
6:     end
7:     if  $\gamma_F < \gamma_{th,F}$  then
8:       Get  $h_m^M, h_m^F$  through FDM;
9:     end
10:    while  $\gamma_m < \gamma_{th,m}$  or  $\gamma_F < \gamma_{th,F}$  do
11:      Get  $A_m, p_F$  through Ruleset( $\gamma_F, \gamma_f, \gamma_m$ );
12:      Virtually take action according to  $A_m, p_F$ ;
13:      Update  $\gamma_F, \gamma_f, \gamma_m$ ;
14:    end
15:  end
16:  Take action according to  $A_m, p_F$ ;
17: end

```

**Algorithm 1** shows the detailed steps of ARLSA. Initially, the access mode of each MUE for the FBS is set to closed (line 1). The algorithm waits until any QoS violation is detected

(line 3). When a violation is detected, the FBS obtains the additional channel information  $h_f^F$  and  $h_f^M$  through the NDM or FDM (line 5 or line 8). Then, ARLSA tries to find a solution in an iterative manner with the information that solves the violation condition (lines 10-14). According to the violation condition and rule sets in **Table 1**, the FBS virtually takes action such as opening the access, adjusting the transmission power, or both (lines 11 and 12). After performing the action, the SINR values are recalculated. If any constraint is not satisfied, further iterations are performed until the constraints are satisfied<sup>4</sup>, and then the FBS takes actual action, i.e., handoff and power adjustment (line 16).

Note that in the iterative loop (lines 10 -14), the action is not actually performed. It is done virtually by ARLSA. After ARLSA finds the final solution which satisfies all of the constraints, each FBS takes action (line 16). Since the action is taken once per violation, ARLSA does not significantly increase the signaling overhead.

For instance, when an FBS is in outage, i.e.,  $\gamma_F \leq \gamma_{th,F}$ , it performs FDM. The FBS obtains the channel state information and determines who is the major interferer, i.e., LN-MUE  $m$ . With the information, the FBS executes an action according to the rule set. If only the FBS constraint is not satisfied, that is, scenario A, the FBS opens its access to the LN-MUE, i.e.,  $A_m = 1$ .

Similarly, when an MUE notices that its QoS requirement is violated, i.e.,  $\gamma_m \leq \gamma_{th,m}$ , the MUE performs NDM and the FBS knows that the MUE is affected by the FBS's transmission. According to the information, this could be either scenario D or F. The FBS performs an appropriate action, i.e., opening the access or controlling the transmission power. In ARLSA, controlling the power means increasing or decreasing the current transmission power of the FBS by  $\Delta p$ . In scenario D, the FBS decreases its FBS power to  $p'_F = p_F - \Delta p$ . Sometimes both FDM and NDM are simultaneously performed, i.e., scenarios E and G. Again, the FBS performs an appropriate action according to the rule set.

Note that when the detected interference comes from another FBS, our proposed ARLSA performed the same manner. That is, the interference is handled by changing association or controlling transmission power of FBSs.

## 5. System Evaluation

In this section, we compare the performance of the proposed KP-IP and ARLSA algorithms with three reference schemes in terms of the throughput and outage. The three reference schemes are i) the power control scheme [6], [7], in which the received powers from both MBS and FBS are made to be equal at a particular point, ii) the open access scheme [3], [12], where the access is granted to nearby MUEs if there are enough resources with the FBS, and iii) the probabilistic scheme, where each FBS decides to open its access with probability 0.5.

### 5.1 Simulation Environment

There is one MBS and many FBSs deployed in its coverage area. The MBS transmission power is fixed while FBSs changes their power according to the power control algorithms in KP-IP, ARLSA, and the power control scheme. FBSs are deployed in the form of the grid

<sup>4</sup> There is another stopping condition for the iteration which is no gain in the network capacity for some number of iterations. We omit this condition in Algorithm 1 to emphasize the main algorithm.

model suggested by 3GPP [22], representing a single floor building with  $10 \text{ m} \times 10 \text{ m}$  apartments. An FBS is deployed in each grid with a particular deployment probability  $p_d$ .

Then, the expected number of FBSs is  $\sum_{k=0}^n k \binom{n}{k} (p_d)^k (1-p_d)^{n-k}$ . Each FBS has four active

FUEs and the MBS has 120 users that are uniformly distributed in the coverage area of the MBS. To capture signal propagation effects, the 3GPP channel models for indoor and outdoor environments are used [22]. The detailed simulation parameters are shown in Table 2.

**Table 2.** Simulation Parameters

Parameters	Value
Bandwidth ( $BW$ )	10 MHz
MBS tx. power	43 dBm
FBS tx. power	between 0 and 25 dBm
Thermal noise density	-174 dBm/Hz
Grid dimensions	10 m $\times$ 10 m
FUEs per FBS	4
Deployment probability ( $p_d$ )	0.1
Min. SINR required (FUE)	0 dB
Min. SINR required (MUE)	0 dB
MUE/FUE tx. power	21 dBm
Number of MUEs	120
BS/UE antenna gain	0 dBi
Wall loss ( $L_w$ )	6.9 dB
Indoor Path-Loss Model	$37 + 32 \log_{10}(R) + L_w$ dB
Outdoor Path-Loss Model	$15.3 + 37.6 \log_{10}(R) + L_w$ dB

$R$  is the distance between BS and UE in meters

## 5.2 Simulation Results

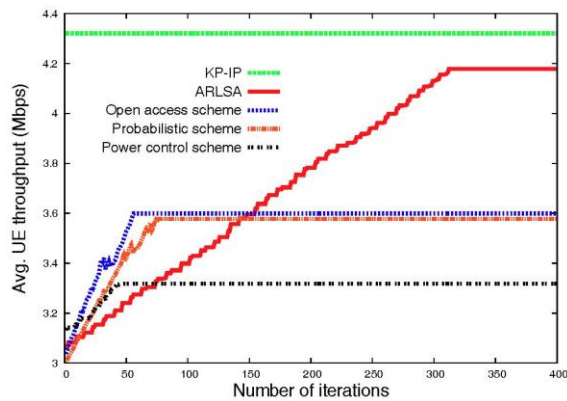


**Fig. 6.** Network-wide throughput according to the number of iteration of local search algorithms

**Fig. 6** shows the average user throughput where the x-axis indicates the number of iterations. The throughput of the KP-IP algorithm is straight line since it is not an iterative algorithm. The KP-IP algorithm shows the best performance, but it is not a practical solution since it is a centralized algorithm and requires the channel gain information of all of the users. The proposed ARLSA performs better than the others, showing 16.1% and 25.9% higher throughput than the open access and power control schemes, respectively. The throughput of ARLSA converges within about 300 iterations.

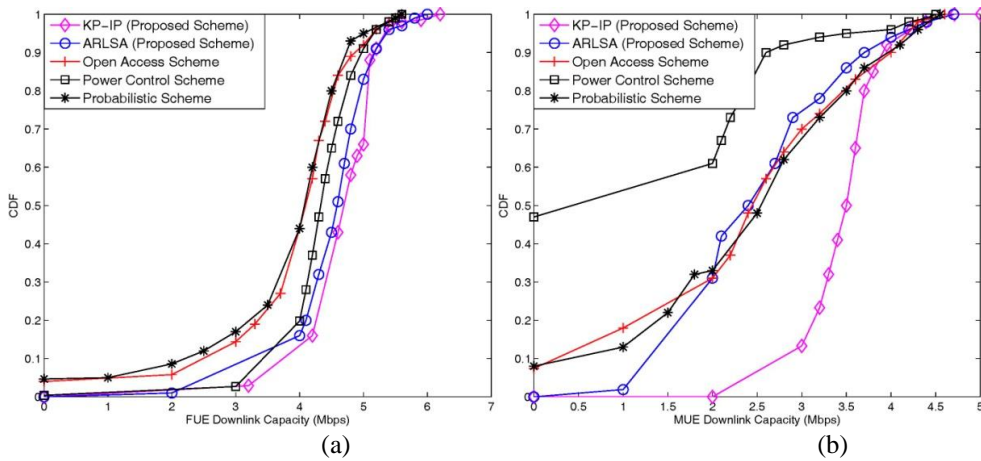


**Fig. 7.** Downlink throughput

**Fig. 7** shows the downlink throughput of the FUE and MUE. For the downlink case, 5% of the FUEs in the open access and probabilistic schemes are in outage since the interference from the MBS to the FUEs cannot be properly mitigated. On the other hand, no FUE is in outage in the power control scheme because it always protects the FUEs by transmitting high power at the FBSs. The proposed scheme does not have any FUEs in outage either and their throughput is higher than that in the other schemes. For the MUE case, **Fig. 7(b)** shows a different result to the FUE case. In the power control scheme, about 50% of the MUEs are in outage since they are not protected from the interference caused by the FBSs. Also, 10% of the MUEs in the open access and probabilistic schemes are in outage. Regardless of the types of FUE and MUE, the proposed schemes perform better in terms of the throughput and outage.

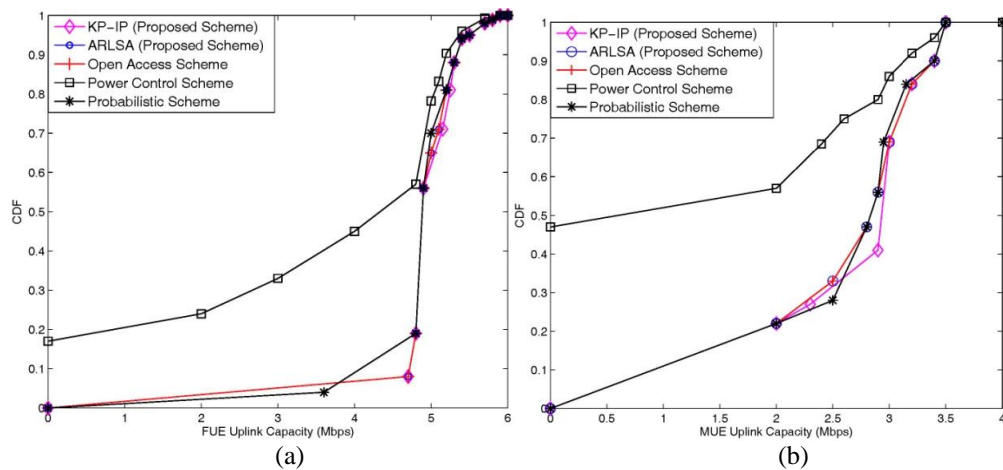


**Fig. 8.** Uplink throughput

**Fig. 8** shows the uplink throughput of the FUE and MUE. The power control scheme has a bad effect on the uplink throughput of the both FUE and MUE, resulting in a high probability of outage. The performances of the proposed, open access, and probabilistic access schemes are comparable.

It is confirmed that the proposed schemes always outperform the three reference schemes in terms of throughput and outage regardless of the uplink and downlink with the same amount of signaling overhead. This means that in a densely deployed network, all of the users cannot be properly served by controlling only parameters such as power or access mode.

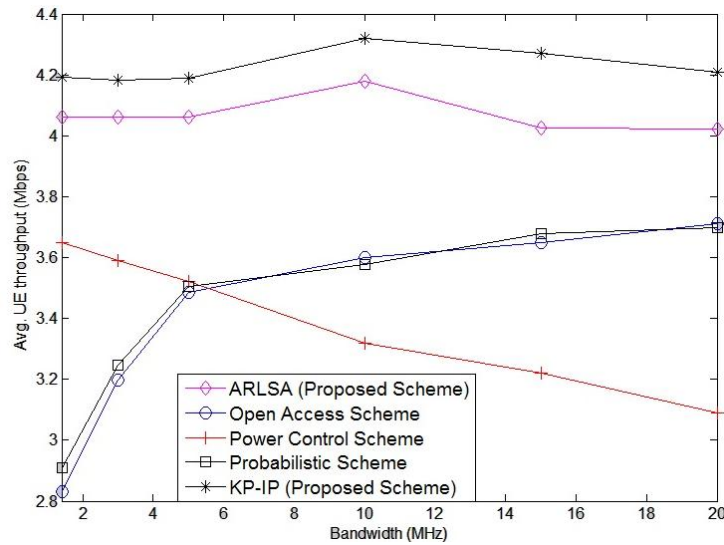


**Fig. 9.** Effects of variable bandwidth on avg. UE throughput

**Fig. 9** shows the effects of variable bandwidth for the proposed and reference schemes. In narrow bandwidths (1.4 MHz and 3 MHz), the power spectral density is high, so the power control scheme shows good performance. On the other hand, the open access scheme in the bandwidths does not perform well since it has limited frequency resource to share with other MUEs. In broad bandwidths (10 MHz, 15 MHz, and 20 MHz), the throughput performance results for the power control and open access schemes are opposite since the power spectral density is low and enough frequency resource to share in the bandwidths. The proposed schemes, i.e., ARLSA and KP-IP, adaptively use both power and association controls, so their performance is not affected according to the bandwidth range. Again, KP-IP shows the best performance for all cases.

### 5.3 Backhaul Signaling Overhead and Latency

Some signaling overhead over the backhaul is induced by the interference detection procedures. If an N-MUE initiates the feedback procedure, the message overhead would be  $b_{ID} + 2b_{RSS}$ , where  $b_{ID}$  and  $b_{RSS}$  are the MUE's ID and RSSs ( $h_m^M$  and  $h_m^F$ ), respectively. When an FBS detects interference, it transmits its own PCI to the MBS over the backhaul. Then, the MBS returns information, that is, the MUE's ID and RSSs ( $h_m^M$  and  $h_m^F$ ). The exchanging message size would be  $b_{ID} + 2b_{RSS} + b_{PCI}$ , where  $b_{ID}$  is 16 bits in our simulations [25], and  $b_{RSS}$  needs 8 bits to represent the different levels of received signal

strength [26], and  $b_{PCI}$  is 9 bits.

Let us suppose an extreme case where all of the FBSs experience cross-tier interference. In our simulations, there are around 60 FBSs. Then, the total overhead is  $60(16 + 2 \cdot 8 + 9) = 2460$  bits, which is negligible in a practical network. The femtocells use the Internet as their backhaul, so the signaling delay may not be strictly bounded. Considering that the average network latency between two different cities in the USA is about 35 ms [27], the self-configuration time of several seconds is sufficient to take all the steps required for cross-tier interference mitigation.

#### 5.4 Execution Time

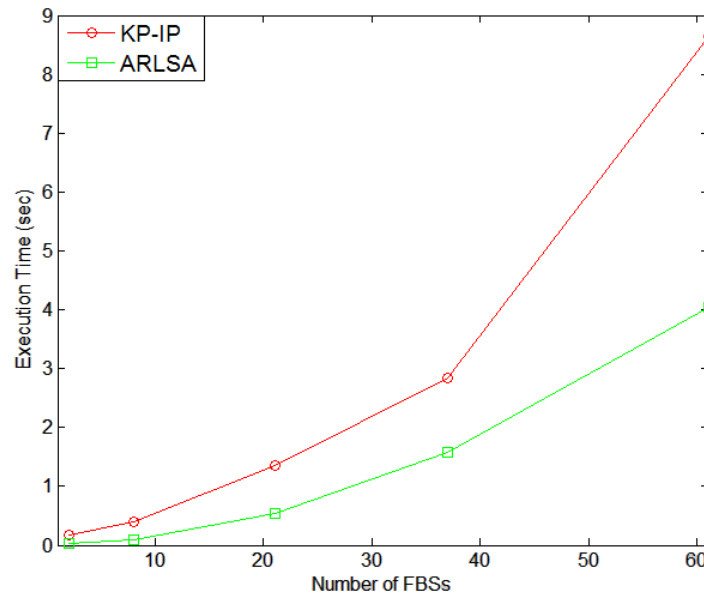


**Fig. 10.** Execution time for KP-IP and ARLSA algorithms according to the number of FBSs

The execution times for the whole iterations of the KP-IP and ARLSA algorithms according to the number of FBSs are shown in Fig. 10. We can infer the computational complexity from the execution time. The hardware platform of the simulation server is an Intel Core i7-4770 running at 3.40 GHz with 8 GB of RAM, and its OS is Windows 7 64-bit. Each FBS has four FUEs and the number of MUEs is twice the number of FBSs. It is confirmed that the execution time of the KP-IP and ARLSA increases exponentially with the number of FBSs. However, since the execution time of ARLSA in the figure is an aggregated value for all FBSs, the execution time of ARLSA for an FBS should be divided by the number of FBSs, resulting in a linear increase with increasing number of FBSs. Therefore, the KP-IP algorithm might not provide a solution in real time for densely deployed femtocell networks while ARLSA always provides a solution.

## 6. Conclusion

Femtocells are one of the most prominent solutions for the high data demand of indoor users. However, they inevitably suffer from cross-tier interference due to the unplanned deployment of the FBSs by customers. To solve this problem, this paper proposed a joint access and power

control scheme for uplink and downlink transmissions which runs at each FBS in a distributed manner. The proposed scheme consists of two parts: the interference detection part and adaptive rule based local search algorithm (ARLSA). With the interference information, ARLSA tries to satisfy QoS constraints of the FUE, MUE, and FBS. Through extensive simulations, it is shown that ARLSA performs 25.9% and 16.1% better than the existing power and access control schemes, respectively. Since the backhaul signaling overhead and computational complexity in our scheme is reasonably low, ARLSA is applicable to real femtocell networks.

## References

- [1] "Cisco Visual Networking Index: Global Mobile Data Traffic Forecast Update, 2014-2019 White Paper," Feb. 2015, available: [http://www.cisco.com/c/en/us/solutions/collateral/service-provider/visual-networking-index-vni/white\\_paper\\_c11-520862.pdf](http://www.cisco.com/c/en/us/solutions/collateral/service-provider/visual-networking-index-vni/white_paper_c11-520862.pdf) [Accessed: Sep. 2015].
- [2] J. Zhang and G. de la Roche, *Femtocells: Technologies and Deployment*, John Wiley and Sons, LTD., Mar. 2010. [Article \(CrossRef Link\)](#).
- [3] D. Choi, P. Monajemi, S. Kang, and J. D. Villasenor, "Dealing with Loud Neighbors: The Benefits and Tradeoffs of Adaptive Femtocell Access," in *Proc. IEEE GLOBECOM*, Nov.-Dec. 2008. [Article \(CrossRef Link\)](#).
- [4] T. Lee, H. Kim, J. Park and J. Shin, "An Efficient Resource Allocation in OFDMA Femtocells Networks," in *Proc. IEEE VTC-Fall*, Sep. 2010. [Article \(CrossRef Link\)](#).
- [5] A. Ruihong, Z. Xin, C. Gen, Z. Ruiming and S. Lin, "Interference Avoidance and Adaptive Fraction Frequency Reuse in Hierarchical Cell Structure," in *Proc. IEEE WCNC*, Apr. 2010. [Article \(CrossRef Link\)](#).
- [6] M. S. Kim, H. W. Je and F. A. Tobagi, "Cross-tier Interference Mitigation for Two-tier OFDMA Femtocell Networks with Limited Macrocell Information," in *Proc. IEEE GLOBECOM*, Dec. 2010. [Article \(CrossRef Link\)](#).
- [7] H. Claussen, T.W. Lester and L.G. Samuel, "Self Optimization of Coverage for Femtocell Deployments," in *Proc. IEEE WTS*, Apr. 2008. [Article \(CrossRef Link\)](#).
- [8] S. Guruacharya, D. Niyato, D.I. Kim and E. Hossain, "Hierarchical Competition for Downlink Power Allocation in OFDMA Femtocell Networks," *IEEE Trans. On Wireless Comm.*, Vol. 12, No. 4, April 2013. [Article \(CrossRef Link\)](#).
- [9] V. Chandrasekhar, J. G. Andrews, T. Muharemovic, Z. Shen and A. Gatherer, "Power Control in Two-Tier Femtocell Networks," *IEEE Trans. On Wireless Comm.*, Vol. 8, No. 8, Aug. 2009. [Article \(CrossRef Link\)](#).
- [10] Y. S. Soh, T. Q. S. Quek, M. Kountouris and G. Caire, "Cognitive Hybrid Division Duplex for Two-Tier Femtocell Networks," *IEEE Trans. on Wireless Comm.*, Vol. 12, No. 10, Oct. 2013. [Article \(CrossRef Link\)](#).
- [11] G. de la Roche, A. Valcarce, D. Lopez-Perez and J. Zhang, "Access Control Mechanisms for Femtocells," *IEEE Commun. Mag*, Jan. 2010. [Article \(CrossRef Link\)](#).
- [12] D. Lopez-Perez, A. Valcarce, G. de la Roche, E. Liu and J. Zhang, "Access Methods to WiMAX Femtocells: A Downlink System-level Case Study," in *Proc. IEEE ICCS*, Nov. 2008. [Article \(CrossRef Link\)](#).
- [13] P. Xia, V. Chandrasekhar and J. G. Andrews, "Open vs. Closed Access Femtocells in the Uplink," *IEEE Trans. On Wireless Comm.*, Vol. 9, No. 12, Dec. 2010. [Article \(CrossRef Link\)](#).
- [14] X. Ge, T. Han, Y. Zhang, G. Mao, C-X. Wang, J. Zhang, B. Zhang and S. Pan, "Spectrum and Energy Efficiency Evaluation of Two-Tier Femtocell Networks with Partially Open Channels," *IEEE Trans. on Veh. Tech.*, Vol. 63, No. 3, March 2014. [Article \(CrossRef Link\)](#).
- [15] J. J. Fruin, "Pedestrian Planning and Design," Metropolitan Association of Urban Designers and Environmental Planners, New York, 1971.

- [16] H. Kellerer, U. Pferschy and D. Pisinger, *Knapsack Problems*, Springer, 2004. [Article \(CrossRef Link\)](#).
- [17] S. Boyd and L. Vandenberghe, *Convex Optimization*, Cambridge University Press, 2004. [Article \(CrossRef Link\)](#).
- [18] Mathworks, “Binary Integer Programming Algorithms,” available: <http://www.mathworks.com/matlabcentral/fileexchange/95-bnb> [Accessed: Sep. 2015].
- [19] K. Han and S. Choi, A study on Self-Organization Strategies for Femtocell Networks, available: <http://dcollection.snu.ac.kr/jsp/common/DcLoOrgPer.jsp?sltItemId=000000029024> [Accessed: Sep. 2015].
- [20] R. Vanderbei and D. Shanno, “An Interior-point Algorithm for nonconvex Nonlinear Programming,” *Computational Optimization and Applications*, Vol. 13, Apr. 1999. [Article \(CrossRef Link\)](#).
- [21] “Interior Point Methods,” <http://www.math.umbc.edu/~potra/talk0930.pdf> [Accessed: Sep. 2015].
- [22] 3GPP TR. 36.922, “Evolved Universal Terrestrial Radio Access (E-UTRA); HeNB RF Requirements,” Sep. 2014. available: <http://www.3gpp.org/dynareport/36922.htm> [Accessed: Sep. 2015].
- [23] H. Holma and A. Toskala, *LTE for UMTS OFDMA and SC FDMA based Radio Access*, John Wiley and Sons, LTD., 2009. [Article \(CrossRef Link\)](#).
- [24] Alexander Gerdenitsch, System Capacity Optimization of UMTS FDD Networks, available: [http://www.nt.tuwien.ac.at/mobile/theses\\_finished/PhD\\_Gerdenitsch/paper.pdf](http://www.nt.tuwien.ac.at/mobile/theses_finished/PhD_Gerdenitsch/paper.pdf) [Accessed: Sep. 2015].
- [25] S. Sesia, I. Toufik and M. Baker, *LTE - The UMTS Long Term Evolution: From Theory to Practice*, 2nd Edition, John Wiley and Sons, LTD., Jul. 2011. [Article \(CrossRef Link\)](#).
- [26] D. Lopez-Perez, A. Valcarce, A. Ladanyi, G. de la Roche and J. Zhang, “Intracell Handover for Interference and Handover Mitigation in OFDMA Two-tier Macrocell-Femtocell Networks,” *Eurasip J. Wireless Commun. and Netw.*, 2010. [Article \(CrossRef Link\)](#).
- [27] L. Ciavattone, A. Morton and G. Ramachandran, “Standardized Active Measurements on a Tier 1 IP Backbone,” *IEEE Comm. Mag.*, vol. 41, no 6, Jun. 2003. [Article \(CrossRef Link\)](#).



**Mujeeb Ahmed** received the M.S. degree in Electrical Engineering from Seoul National University, Seoul Korea, in 2012. He is currently pursuing Ph.D. degree at the Information Systems Technology and Design Pillar, Singapore University of Technology and Design. His research interests include security in cyber physical systems mainly, in infrastructures like IoT, smart grid and water treatment systems.



**Sung-Guk Yoon** received the B.S. and Ph.D. degrees from Seoul National University, Seoul Korea, in 2006 and 2012, respectively. From 2012 to 2014, he was a Postdoctoral Researcher at the same university. He is currently with Sonngsil University as an Assistant Professor since March 2014. His research interests include smart grid and power line communications.